Journal of Nanoparticle Research (2005) 7: 219–225
DOI: 10.1007/s11051-005-2500-6

Temperature dependent structural and optical properties of nanocrystalline CdO thin films deposited by sol–gel process

P.K. Ghosh, S. Das and K.K. Chattopadhyay
Department of Physics, Thin Film & Nano Science Lab, Jadavpur University, Kolkata 700 032, India (E-mail: kkc@juphys.ernet.in)

Received 12 November 2004; accepted in revised form 18 February 2005

Key words: CdO-nanoparticles, temperature dependence, sol–gel, TEM, XRD, optical

Abstract

Nanocrystallites of cadmium oxide (CdO) thin films were deposited by sol–gel dip coating technique on glass and Si substrates. XRD and TEM diffraction patterns confirmed the nanocrystalline cubic CdO phase formation. TEM micrograph of the film revealed the manifestation of nano CdO phase with average particle size lying in the range 1.6–9.3 nm. UV–Vis spectrophotometric measurement showed high transparency (nearly 75% in the wavelength range 500–800 nm) of the film with a direct allowed bandgap lying in the range 2.86–3.69 eV. Particle size has also been calculated from the shift of bandgap with that of bulk value for the films for which the particles sizes are comparable to Bohr exitonic radius. The particle size increases with the increase in annealing temperature and also the intensity of XRD peaks increases which implies that better crystallinity takes place at higher temperature.

Introduction

The preparations of nanometer size crystallites open the opportunity of observing the evolution of physical properties of the materials with sizes. The reduction of sizes with which the bulk properties change remarkably and provide the possibility of observing novel behaviors such as size-dependent structural, electrical and optical properties. The physics associated with these properties of nanocrystallites of II–VI semiconductors have been very interesting because of thinking the phenomena in a new point of view with the properties exhibited by them. Nanocrystalline semiconductors have attracted much attention due to their novel properties and varieties of promising potentials in extensive applications (Bachtold et al., 2001; Huang et al., 2001). Numerous technical advancements in the field of nanostructured materials have stimulated the wide range of research interest in recent years because of various new properties exhibited by them. Recently, nanostructured semiconductors are widely used to design a rich varieties of device for microelectronics. One-dimensional nanostructured materials have gained special interest in the assembly of nanodevices (Bachtold et al., 2001; Huang et al., 2001a,b). Nanometer-scale electronics have been predicted to play an important role in device technology (Pease, 1992; Schon et al., 2001). Quantum wires of semiconductors (Lee et al., 1993) and metallic alloys (Blythe, 2000) have found to exhibit interesting magnetic and electrical properties. The nanostructured transparent conducting oxides have also gained tremendous importance due to their size dependent optical properties and possible applications in near future.

Recently, various research groups around the world are working on the synthesis of several II–VI n-type transparent semiconducting oxide thin films by different processes. Previously, thin films of cadmium oxide (CdO) have been synthesized by various techniques, including activated reactive evaporation (Phatak et al., 1994), spray pyrolysis (Gurumurugan et al., 1994; Sanatana et al., 1999), solution growth (Verkey & Fort, 1994), MOCVD (Freeman et al., 2000), PLD (Yan et al., 2001), rf sputtering (Ueda et al., 1998) etc. Recently, F doped CdO thin film has been reported (Ghosh et al., 2004) via sol–gel process. The preparation of ZnO quantum dots (Mahamuni et al., 1999), nanowires and nanoribbons (Yao et al., 2002), nanorods (Guo et al., 2002; Liu & Zeng, 2003) etc. have been studied widely. The nanostructure of CdO have been prepared (Ashrafi et al., 2002) via metalorganic molecular-beam epitaxy and nanobelts have also been prepared (Pan et al., 2001) via thermal evaporation method. But no more detailed studies of temperature dependent of nanostructural properties such as XRD and TEM have been reported in the literature so far. Here we have studied the temperature dependence of nanostructural and optical properties of CdO thin films deposited via sol–gel dip-coating process. We have chosen the dip-coating method because of its many advantages such as easier composition control, better homogeneity, low processing temperature, lower cost, easier fabrication of large area films, possibility of using high purity starting materials and having an easy coating process of large and complex shaped substrates.

Experimental

Preparation of films by sol–gel

The thin films of CdO have been deposited on glass and Si substrates using sol–gel dip coating process. Cadmium acetate (99.99% $Cd(COOCH_3)_2$) has been taken as the source cadmium and 2-methoxy ethanol and monoethanol amine have been taken as solvent and stabilizer, respectively. The solution of cadmium acetate dissolving in 2-methoxy ethanol was stirred by a magnetic stirrer and heated at a constant temperature of ~80°C for a 1 h. The solution was aged for 3 h. Before dip coating the glass substrates were cleaned by mild soap solution, washed thoroughly by distilled water and then in boiled water. Finally, it was degreased in alcohol vapor. Si substrates were cleaned at first in 20% HF solution for 5 min and then washed in acetone in an ultrasonic cleaner. The cleaned substrates were dipped vertically into the solution and withdrawn very slowly at a speed of ~8 cm/min and dried at 60°C for 15 min for quick gel formation. This process was repeated for eight to nine times. Finally, the coated substrates were annealed at desired constant temperature 200°C, 250°C, 300°C and 350°C for 1 h in open air.

For study of nanostructure by transmission electron microscopy, we prepared the samples as follows: at first, the films (CdO nanoparticles), deposited on glass substrates annealed at different temperature, were scratched out carefully by a sharp knife edge from some portion of the substrates. These particles were dispersed in ethanol by ultrasonication and then a few drop of this solution was placed on carbon-coated copper grid and it was allowed to dry out. For different annealed temperature different carbon coated copper grids were used and the materials on carbon coated copper grid were utilized to measure the TEM image.

Characterization

The nanostructure and the selected area electron diffraction pattern of the films were studied by a transmission electron microscope (TEM, Hitachi-H600). X-ray diffraction pattern was recorded by an X-ray diffractometer (Bruker D8 Advance) in 2θ range 20–70° using Cu K_α radiation of wavelength $\lambda = 0.15406$ nm. It was operated at 40 kV and 40 mA. Fourier-transformed infrared spectroscopy (FTIR, Shimadzu 8400S) was studied in wave number range 400–2000 cm^{-1}. The optical transmission spectra of the films were measured in the wavelength range $\lambda = 300$–800 nm using a UV–VIS–NIR spectrophotometer (Shimadzu UV-3101PC) at room temperature. The thickness of the film (~400 nm) was estimated from cross-sectional scanning electron microscopy (SEM, JEOL-5200) measurement.

Results and discussion

Nanostructural studies and X-ray diffraction

The nanostructure of the films, prepared by dispersing the nanoparticles on carbon-coated copper

grid, were studied at room temperature by using TEM. The micrographs and corresponding diffraction pattern of CdO thin films for different annealing temperature have been shown in Figure 1 (a) 200°C, (b) 250°C, (c) 300°C and (d) selected area electron diffraction (SAED) pattern for temperature 250°C. The SAED of the film consists of central halo and concentric rings and these are almost same for all the films (one of them is shown here). From the diameter of the rings, we calculate the interplaner spacing (d) values, which correspond to reflection from (1 1 1) and (2 2 0) planes of cubic CdO. The average diameter of the particles have been determined from the peak of particle distribution plots (not shown here) of TEM micrographs. The particle size lies in the range 1.6–9.3 nm.

X-ray diffraction patterns of the CdO thin films using CuKα radiation of wavelength $\lambda = 1.5406$ Å has been shown in Figure 2 for different annealed temperature (a) 200°C, (b) 250°C, (c) 300°C and (d) 350°C. The several peaks of cubic face-centered CdO with $a_0 = 4.6953$ Å have been obtained due to diffraction form (1 1 1), (2 0 0), (2 2 0) and (3 1 1) planes. The information on strain (ε) and the particle size (L) of the deposited films have been obtained from the following relation (Quadri et al., 1999):

$$\frac{\beta \cos\theta}{\lambda} = \frac{1}{L} + \frac{\varepsilon \sin\theta}{\lambda}, \tag{1}$$

where β is the Full-Widths-at-Half-Maximum (FWHM) of the diffraction peaks. Figure 3 represents the plot of $\beta \cos\theta/\lambda$ vs. $\sin\theta/\lambda$. Slope of the graph depicts the strain values which lie in the range 0.048–0.024 and the intercept on y-axis gives the crystallite size which lie in the range 2.4–15.4 nm. Figure 4 shows the variation of particle size and strain with annealing temperature. It is clear from the figure that as the annealing temperature increases, the particle size also increases but the strain value decreases. The interplaner spacing (d) corresponding to XRD peaks, TEM measurement and JCPDS card have been compared as shown in Table 1. X-ray diffraction pattern of CdO-nano shows broadening of peaks, which indicate CdO is nanocrystalline in nature.

Figure 5 shows the FTIR spectrum of a CdO thin film deposited on a Si substrate and annealed at 300°C for 1 h. The bands have been assigned to the absorption peaks due to Cd–O, and Si–O bond

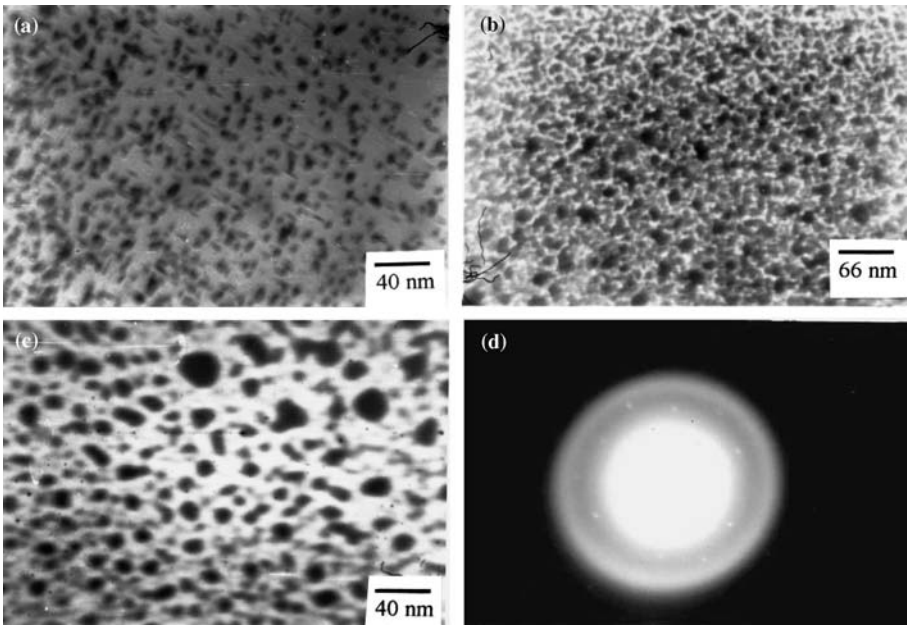

Figure 1. Transmission electron micrographs of nanocrystalline CdO thin films deposited on carbon-coated copper grid at different temperature (a) 200°C, (b) 250°C and (c) 300°C; (d) at 250°C Typical selected area electron diffraction pattern of the thin film.

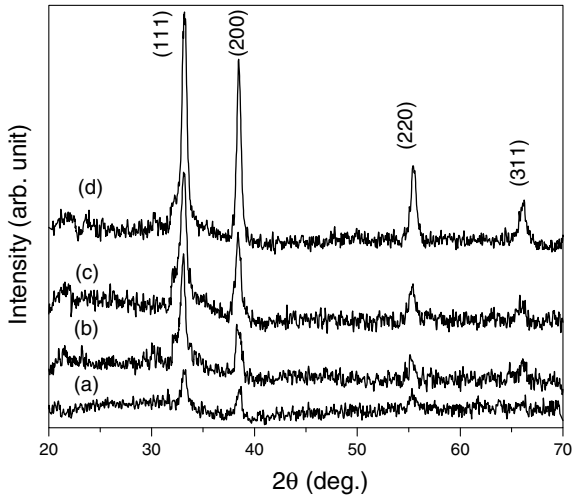

Figure 2. XRD patterns of a nanocrystalline CdO thin films deposited on glass substrates annealed at different temperature (a) 200°C, (b) 250°C, (c) 300°C and (d) 350°C.

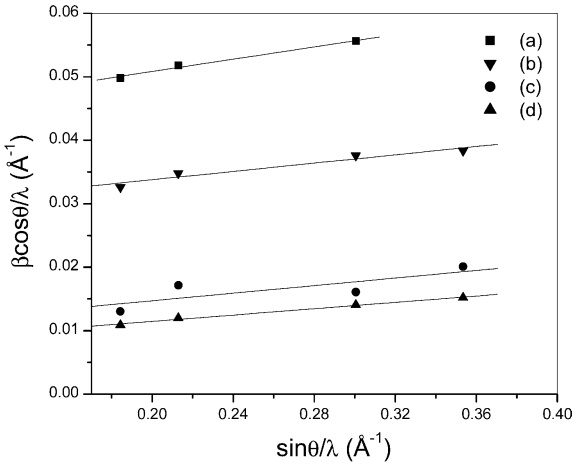

Figure 3. Plot to determine the particle size and strain of nanocrystalline CdO thin films for different annealing temperatures (a) 200°C, (b) 250°C, (c) 300°C and (d) 350°C.

vibrations. The peaks are due to bond vibrational energy of Cd–O at 548 cm^{-1} (Landolt Bornstein, 1987); Si–O at 446 cm^{-1} and 1078 cm^{-1}. The peaks of Si–O bond vibrations have been occurred in the spectrum due to the use of Si substrate, which may be oxidized at the surface because of air annealing of the film. One peak at 493 cm^{-1} remains unassigned.

Optical absorption and optical bandgap

Figure 6 shows the transmittance vs. wavelength traces which show nearly 75% transmittance in the

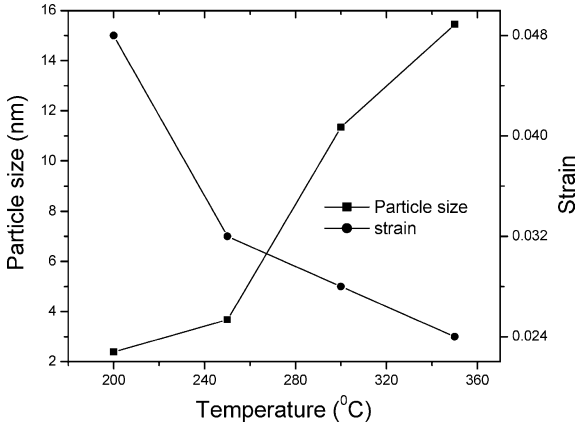

Figure 4. Variation of crystallite size and strain with annealing temperature.

Table 1. Interplaner spacing (*d*) from TEM, XRD and JCPDS data card and corresponding (h k l) values

$d_{(TEM)}$ (Å)	$d_{(XRD)}$ (Å)	$d_{(JCPDS)}$ (Å)	(h k l)
2.71	2.713	2.712	(1 1 1)
2.35	2.349	2.349	(2 0 0)
–	1.660	1.661	(2 2 0)
–	1.415	1.416	(3 1 1)

wavelength range of 500–800 nm. The fundamental absorption, which corresponds to electron excitation from the valance band to conduction band, can be used to determine the nature and value of the optical band gap. The relation between the absorption coefficients (α) and the incident photon energy ($h\nu$) can be written as (Pankove, 1971),

$$(\alpha h\nu)^{1/n} = A(h\nu - E_g), \tag{2}$$

where A is a constant and E_g is the band gap of the material and exponent n depends on the type of transition. For direct allowed $n = 1/2$, indirect allowed transition, $n = 2$, and for direct forbidden, $n = 3/2$. To determine the possible transitions, $(\alpha h\nu)^{1/n}$ vs. $h\nu$ were plotted and corresponding band gap were obtained from extrapolating the straight portion of the graph on $h\nu$ axis. The direct bandgap calculated from $(\alpha h\nu)^2$ vs. $h\nu$ plots (as shown in Figure 7) lie in the range 2.86–3.69 eV and indirect bandgap calculated from $(\alpha h\nu)^{1/2}$ vs. $h\nu$ plots lie in the range 1.98–2.44 eV as shown in Figure 8. Both the direct bandgap and indirect bandgap values of the films are higher than that of the value of bulk

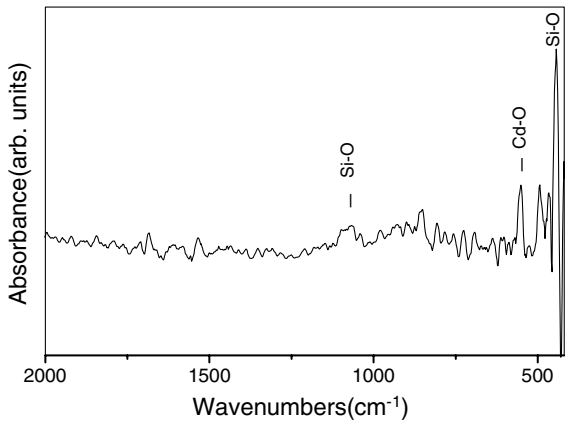

Figure 5. FTIR spectrum of the nanocrystalline CdO thin film deposited on Si substrate annealed at 300°C.

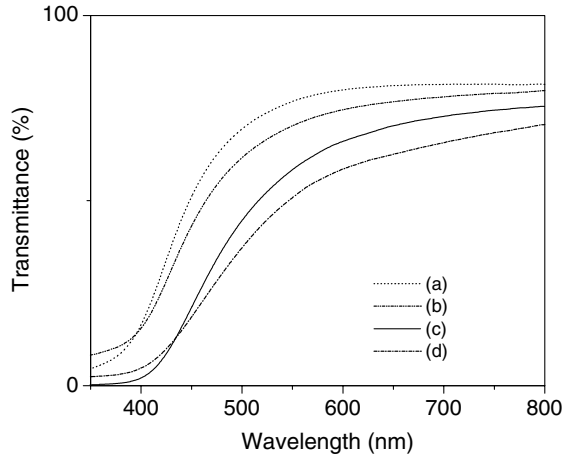

Figure 6. Transmittance spectra of a representative nanocrystalline CdO thin films deposited on glass substrates at different annealed temperatures (a) 200°C, (b) 250°C, (c) 300°C and (d) 350°C.

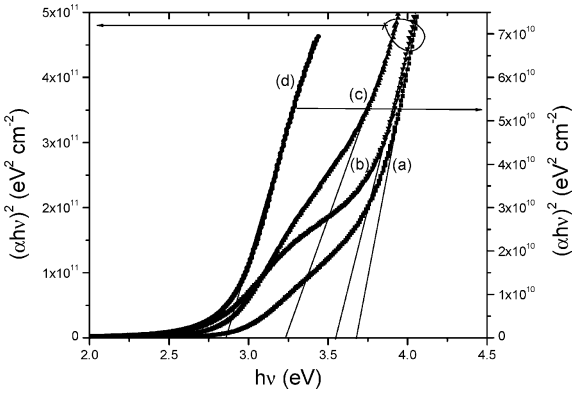

Figure 7. Determination of direct band gap of nanocrystalline CdO thin films for different annealing temperatures (a) 200°C, (b) 250°C, (c) 300°C and (d) 350°C.

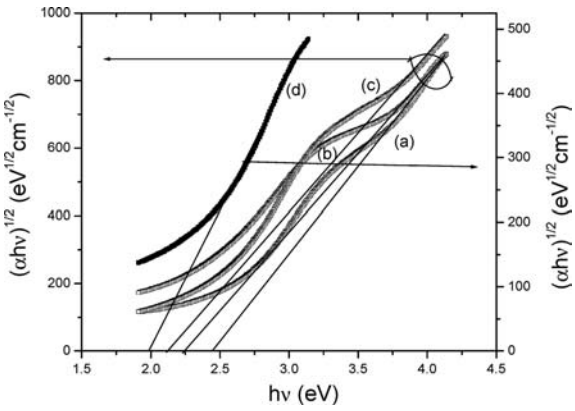

Figure 8. Determination of indirect band gap of nanocrystalline CdO thin films for different annealing temperatures (a) 200°C, (b) 250°C, (c) 300°C and (d) 350°C.

materials because of quantum confinement of CdO nanocrystals.

Figures 7 and 8 have two linear segments. Therefore, there may be more than one interband-absorptions for these nanocrystalline CdO samples. These might be due to the fact that for nanoparticles (size ~few nm) as surface to volume ratio increases, so defect states increase due to increase of surface area and strain than that of bulk CdO. These defects create states at different energies in the forbidden gap and there may be some finite transition probabilities from these states. Hence due to the absorption of energy by the defect states situated at different energies within the forbidden region (for our nanocrystalline CdO thin films), we get different linear segments in Figures 7 and 8.

The properties of nanocrystalline materials are changed from their corresponding bulk properties due to the crystallite size become comparable to the Bohr excitonic radius (r_B).

$$r_B = h^2\varepsilon[1/m_e^* + 1/m_h^*]/\pi e^2, \quad (3)$$

where ε is the permittivity of the sample, m_e^* and m_h^* are the effective mass of electron and hole in

CdO, respectively. The values of the particle size of the CdO thin films, as obtained from TEM studies for annealed temperature below 300°C, are comparable to the Bohr excitonic radius supporting the quantum size effect.

The blue shift of band gap might also be utilized in determining the crystallite radius (r) using relation (Yoffe, 1993; Yuang et al., 1994)

$$\Delta E_g = E_{g(film)} - E_{g(bulk)} = [h^2/8\mu r^2] - [1.8e^2/r\varepsilon] \quad (4)$$

where μ is the reduced mass of electron–hole effective mass and ε is the dielectric constant. From the above equation, the particle sizes have been determined and these lie in the range 2.56–4.06 nm and that obtained from TEM measurements (bellow annealing temperature 300°C) are also fairly support these results.

Table 2 shows the variation of direct bandgap, indirect bandgap and particle size which was obtained from the shift of direct bandgap with different annealed temperatures. It is clear from the Table 2 that the particle size increases with increase in annealed temperature. The increase in particle size with annealed temperature may be due to the coalescence of nanoparticles.

The variation of direct bandgap and indirect bandgap with different annealing temperature are shown in Figure 9. It is clear from this figure that both the direct bandgap and indirect bandgap decreases with increase in annealing temperature. These may be due to better quantum confinement at comparatively lower annealing temperature. Although CdO is a direct band gap material but for nanocrystalline CdO, due to increase of surface to volume ratio of the particles, the defect states increase due to increase of surface area and also strain from that of bulk CdO. These defects actually alter the band diagram and band gap fluctuation over some mean value takes place (Szcyrbowski, 1979; Gavrilenko, 1987). This will create some finite probabilities of indirect transitions in this material. Hence although CdO is a direct band gap material there is still some finite probabilities of observing indirect band gap. Again as annealing temperature increases, particle size increases, so the surface to volume ratio decreases and better crystallinity take place which leads to decrease in defect states. Hence the probability of indirect transition decreases leading to decrease in indirect bandgap energy value.

Conclusion

The thin films of CdO nanoparticles have been successfully prepared by sol–gel process. XRD and SAED patterns confirmed the nanocrystalline cubic CdO phase formation. The XRD peaks are more broaden at lower temperature which indicate that the quantum confinement is better at lower temperature. TEM and optical studies also

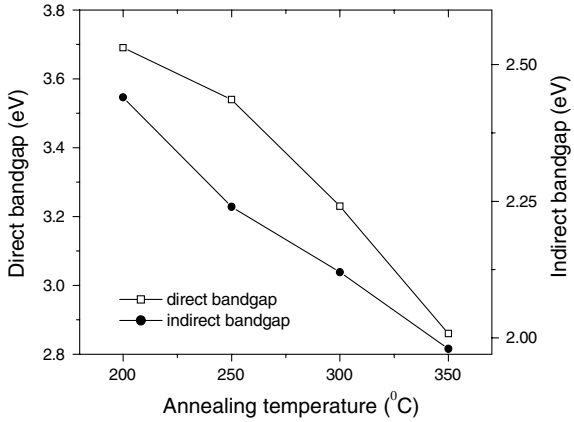

Figure 9. Variation of direct bandgap and indirect bandgap of nanocrystalline CdO thin film with annealing temperature.

Table 2. Comparison of direct bandgap, indirect bandgap and particle size obtained from shift of direct bandgap with different annealing temperature

Name of the sample	Annealing temperature (°C)	Direct bandgap (eV)	Indirect bandgap (eV)	Particle size (nm)
(a) cd-3	200	3.69	2.44	2.56
(b) cd-5	250	3.54	2.24	2.71
(c) cd-9	300	3.23	2.12	3.12
(d) cd-13	350	2.86	1.98	4.06

revealed that the quantum size effect occurred in the films. The particle size obtained from TEM measurement lies in the range 1.6–9.3 nm. Optical transmission spectrum showed nearly 75% transmittance in the wavelength range of 500–800 nm and high direct bandgap lies in the range 2.86–3.69 eV. The indirect bandgap of the films (lies in the range 1.98–2.44 eV) are also higher than that of the bulk CdO materials. This may be due to quantum confinement effect of CdO nanoparticles.

Acknowledgements

The authors wish to gratefully acknowledge the University Grants Commission, Govt. of India, for financial support under the scheme 'University with potential for excellence'. One of us (SD) wishes to thank UGC for awarding him a junior research (JRF) fellowship during the execution of the work.

References

Ashrafi A.B.M.A., I. Suemune, Y.W. Ok & T.Y. Seong, 2002. J. Crystal Growth 237–239, 518.

Bachtold A., P. Hadley, T. Nakanishi & C. Dekker, 2001. Science 294, 1317.

Blythe H.J., V.M. Fedosynk, O.I. Kasyutich & W. Schwarzacher, 2000. J. Magn. Magn. Mater. 208, 251.

Freeman A.J., K.R. Poeppelmeier, T.O. Mason, R.P.H. Chang & T.J. Marks, 2000. MRS Bull. 25, 45.

Gavrilenko K.O., 1987. Phys. Status Solid. B 139, 457.

Ghosh P.K., R. Maity & K.K. Chattopadhyay, 2004. Sol. Energy Mat. Sol. Cells 81, 279.

Gurumurugan K., D. Mangalaraj & S.K. Narayandass, 1994. Thin Solid Films 251, 7.

Guo L., Y.L. Ji, H. Xu, P. Simon & Z. Wu, 2002. J. Am. Chem. Soc. 124, 14864.

Huang M.H., S. Mao, H. Feick, H.Q. Yan, Y.Y. Wu, H. Kind, E. Weber, R. Russo & P.D. Yang, 2001a. Science 292, 1897.

Huang Y., X.F. Duan, Q.Q. Wei & C.M. Lieber, 2001b. Science 291, 851.

JCPDS file card 5 – 0640.

Landolt Bornstein, 1987. New Series Publisher: Springer Verlag.

Lee S.T., Y.F. Zhang, N. Wang, Y.H. Tang, I. Bello, C.S. Lee & Y.W. Chung, 1993. J. Mater. Res. 14, 4503.

Liu B. & H.C. Zeng, 2003. J. Am. Chem. Soc. 125, 4430.

Mahamuni S., K. Borgohain, B.S. Bendre, V.J. Leppert & S.H. Risbud, 1999. J. Appl. Phys. 85, 2861.

Pankove 1971. Optical Processes in Semiconductors, Prentice-Hall.Inc.

Pan Z.W., Z.R. Dai & Z.L. Wang, 2001. Science 291, 1947.

Pease R.F. 1992. In: Kirk W.P. and Reed M.A. eds. Nanostructures and Mesoscopic Systems. Academic, NewYork, p. 37.

Phatak G. & R. Lal, 1994. Thin Solid Films 245, 17.

Quadri S.B., E.F. Skelton, D. Hsu, A.D. Dinsmore, J. Yang, H.F. Gray & B.R. Ratna, 1999. Phys. Rev. B 60, 9191.

Sanatana G., A.M. Acevedo, O. Vigil, F. Cruze, G. Contreras-puente & L. Vaillant, 1999. Superficiesy Vacio 9, 300.

Schon J.H., O. Schenker & B. Batlogg, 2001. Thin Solid Films 385, 271.

Szcyrbowski J.J., 1979. Phys. Status Solid. B 96, 769.

Ueda N., H. Meada, H. Hosono & H. Kawazoe, 1998. J. Appl. Phys. 84, 6174.

Verkey A. & A.F. Fort, 1994. Thin Solid Films 239, 211.

Yan M., M. Lane, C.R. Kannewurf & R.P.H. Chang, 2001. Appl. Phys. Lett. 78, 2342.

Yao B.D., Y.F. Chan & N. Wang, 2002. Appl. Phys. Lett. 81, 757.

Yoffe A.D., 1993. Adv. Phys. 42, 173.

Yuang Y.S., F.Y. Chen, Y.Y. Lee & C.L. Liu, 1994. Jpn. J. Appl. Phys. 76, 3041.